On-line sensing and estimation of laser surface modification by computer vision

D Hu, M Labudovic and **R Kovacevic***
Research Center for Advanced Manufacturing, Southern Methodist University, Richardson, Texas, USA

Abstract: Laser surface modification with alloying or remelting often yields unstable results. To achieve on-line control, process sensing and estimation are the key technologies. This paper introduces molten pool imaging as laser processing feedback. Well-contrasted molten pool images are acquired in experiments by eliminating the strong light from spatter and plasma. An algorithm for real-time image processing is developed that shows robust and high-speed performance. Analytical models of laser surface modification are studied using moving heat source models. The simplified analytical model shows a roughly linear relationship between laser power and depth of modified surface (molten depth). Based on key feature analysis in analytical models, an on-line estimation model of molten depth is built using a neural network, which applies a time- series of widths of the molten pools as an input vector. By controlling laser power, the neural network model is trained for different heat inputs in a transient process. The testing results by another group of experiments show that the on-line estimation model can predict the depth of the modified surface accurately.

Keywords: laser surface modification, on-line estimation, computer vision, image processing, neural network

NOTATION

a	thermal diffusivity (m^2/s) $= k/(\rho c_p)$
$\boldsymbol{a}^m$	output vector of the mth layer of the neural network
$\boldsymbol{b}^m$	bias vector of the mth layer of the neural network
c_p	specific heat (J/kg K)
E	edge set
$\boldsymbol{f}^m$	transfer function of the mth layer of the neural network
G	two-dimensional Gaussian filter
G_n	first derivative of the Gaussian operator
i, j	coordinates of the image array
I, I_s, I_r	image arrays in different processing stages
I_e	edge candidate
k	thermal conductivity (W/m K)
n	normal of the detected edge
$p(t)$	width of the molten pool at time t
$\boldsymbol{P}$	input vector of the neural network
Q	heat rate (W)
r	radius (m) $= (x^2 + y^2 + z^2)^{1/2}$
R	dimension of the input vector of the neural network
S^m	dimension of the output vector of the mth layer of the neural network
T	temperature (K)
T_{e1}, T_{e2}	edge magnitude thresholds
T_{g1}, T_{g2}	grey level thresholds
w	moving speed (m/s)
$\mathbf{W}^m$	weight matrix of the mth layer of the neural network
x, y, z	coordinate system as in Fig. 1
ρ	density (kg/m^3)
σ	Gaussian distribution parameter

The MS was received on 12 November 1999 and was accepted after revision for publication on 19 September 2000.
**Corresponding author: Research Center for Advanced Manufacturing, Southern Methodist University, 1500 International Parkway, Suite 100, Richardson, TX 75081, USA.*

1 INTRODUCTION

Laser surface modification comprises a family of methods such as transformation hardening, melting, alloying and cladding. It allows a user to build a part with totally different properties in the surface layer than in the bulk material. The surface layer can obtain high wear, fatigue or erosion resistance, while the bulk material maintains its original properties, such as good strength.

The theory of laser surface modification is based on rapid thermal cycling due to the ability of the laser to produce concentrated heat energy on the part. A high cooling rate can be reached as the heat conducts into the cold bulk material, which results in a self-quenching process. This self-quenching process produces microstructure refinement, phase transformation or formation of a supersaturated solid solution [**1**].

One typical application of laser surface modification is the thermochemical treatment of the surface of titanium which has excellent mechanical and chemical properties such as high strength, good biocompatibility and high corrosion resistance, but has low resistance to sliding and abrasive wear. When nitrogen is blown into the molten pool produced by the laser on titanium material, a thin golden layer of titanium-nitride forms which shows great hardness (HV = 2000–3000 kg/mm^2), high melting temperature, high temperature stability and low electrical sensitivity [**2**]. However, irregular qualities are often produced because the processes are too sensitive to the processing parameters such as input laser power and scanning velocity. For example, under certain conditions a 10 per cent fluctuation in laser absorption will cause a 50 per cent change in molten depth. Therefore, real-time control of the process is required to produce a more stable and repeatable molten depth and to adapt to the complex shape of the part.

Accurate and reliable process sensing and feedback are the key to achieving such successful control. Owing to the complex interaction between laser and material, there are several kinds of sensor to be used in laser welding to monitor the welding process (e.g. plasma detector, acoustic sensor, spatter detector, temperature probe and keyhole imager [**3**, **4**]) in order to estimate the welding penetration. A few studies have also been carried out on laser surface modification, in which thermal pictures are acquired and analysed to estimate molten depth [**2**, **5**]. Still, sensing the laser process remains a problem to be solved. Owing to the intense light produced by plasma and spatter, direct molten pool imaging is not an efficient method for sensing in the laser surface modification process.

There are also quite a number of research studies on laser processing models, but most of them are numerical and cannot be utilized efficiently to direct real-time process control. An analytical model that is faster and can be applied in real-time control usually depends on the method of sensing. Because of the limitation of the known methods of sensing, there are few research studies on on-line estimation. Among them, Lankalapalli and Tu [**6**] developed an analytical model for keyhole laser welding by assuming a constant temperature in the keyhole and applying a moving line heat source model. Romer and Meijer [**7**] provide an analytical model for laser surface modification based on thermal pictures, but some hypotheses (such as bead width) conflict with observed experimental results of the present authors.

In this study, an ultrahigh-speed shutter camera with pulsed laser illumination (known as the Laser Strobe vision system) has been used as the laser process monitor, which is able to acquire well-contrasted images of the molten pool. Owing to the large amount of adjustments and experiments, stainless steel AISI 304 was chosen as the treatment material in the preliminary experiments for economical reasons. The sensing and estimation method certified for stainless steel can be extended to titanium material in future work. The experimental results show that there is a clear correlation between molten depth, molten pool size and geometric shape during constant scan velocity processing. A real-time algorithm of image processing has been developed to calculate the molten pool geometric parameters, which performs well because it is robust and fast. Analytical models of moving heat sources of point and Gaussian distribution have been discussed to explore the relation between laser power and molten depth, and to decide the key features for neural network model training. Based on analysis in analytical models, an on-line molten depth estimation model is built using the neural network and is trained with the back propagation method.

In the next section, the system set-up and preliminary experiment results are illustrated, showing a rough correlation between processing parameters and the molten pool geometric shape. A real-time algorithm of image processing is provided in the third section. Analytical models of the moving heat source are discussed in the fourth section. The analytical model of the moving point heat source demonstrates an approximate linear relationship between the laser power absorbed and the depth of surface modification. Based on analysis of the key features in analytical models, in the fifth section, a neural network on-line estimation model is built using a multilayer perceptron (MLP) and trained by the back propagation training method. The conclusions are presented in the final section.

2 PRELIMINARY EXPERIMENTS

In order to certify whether or not the image of the molten pool is an efficient information source to reflect the molten depth, while trying to find the potential correlation between molten depth and the molten pool geometric shape, a series of preliminary experiments have been performed using different pairs of laser powers and scan velocities as processing parameters. An Nd:YAG laser is the laser source, which is operated in continuous waveform (CW) mode. Owing to the large amount of adjustments and experiments, stainless steel AISI 304 was chosen as the treatment material at the beginning for economical reasons. The sensing and estimation method certified in this study will be extended to titanium in future work.

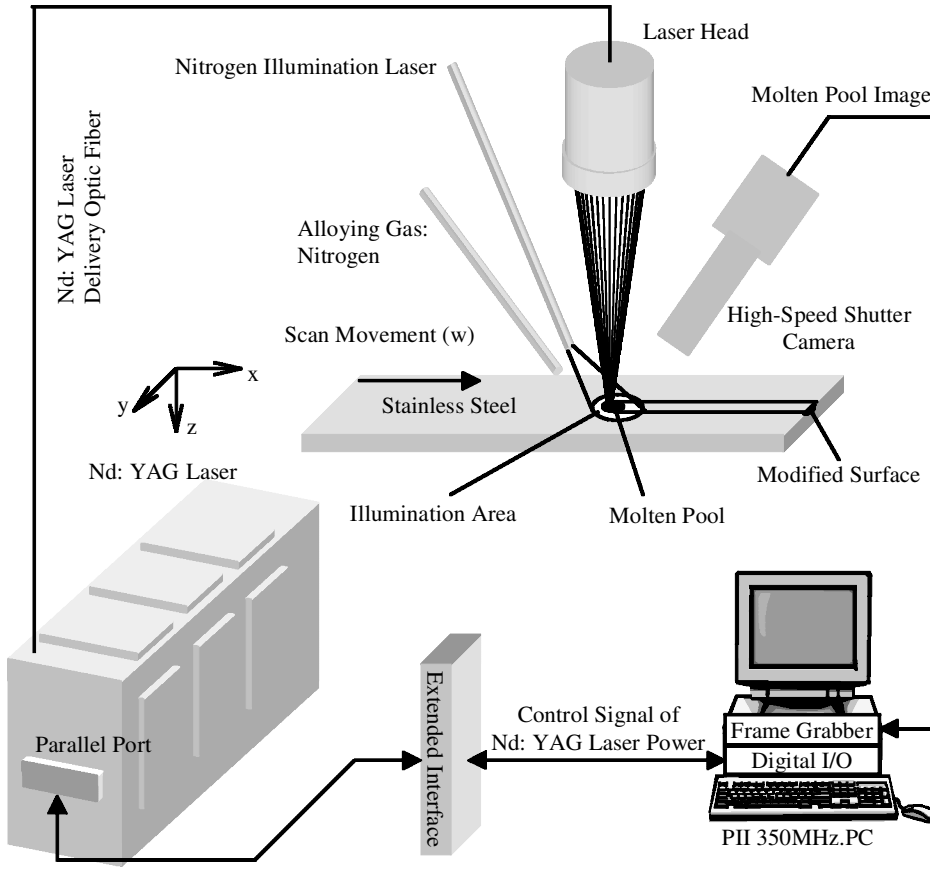

Fig. 1 Experimental system set-up

Figure 1 gives the experiment system set-up. Laser fibre conducts a 337 nm near-UV laser to illuminate the Nd:YAG laser treating area. The illuminating laser is a pulse laser with a 5 ns pulse duration synchronized with the high-speed shutter of the camera. The camera is also equipped with a UV filter that only allows light near 337 nm wavelength to pass. As the illuminating laser is triggered, the camera shutter opens for 50 ns to capture an image. During the illumination period, the intensity of the illuminating laser can cover the spatter and plasma light. Owing to the reflection of the mirror-like molten pool, a well-contrasted image of the molten pool can be obtained. Nitrogen is used as the alloying gas; it also blows away the plasma generated from the molten pool. A frame grabber installed on a PII 350 PC computer acquires images from the high-speed shutter camera at 30 Hz. Real-time image processing, molten depth on-line estimation and closed-loop control will be completed on the same computer. A digital I/O card is also mounted on the same PC to control the power of the MW-1000 Nd:YAG laser through its parallel port using an extended interface. The experiment results using constant processing parameters are shown in Figs 2 and 3.

With a laser strobe lighting camera, well-contrasted molten pool images can be acquired, the quality of which is sufficient for further image processing. From data in Fig. 2, the depth of the modified surface shows more sensitivity to absorbed laser power than to scan velocity. For example, processing started with parameters of 1200 W laser power and 2.5 mm/s scan velocity. Decreasing the laser power by 50 per cent or increasing the scan speed by 300 per cent will form almost the same variation in depth in the molten pool. Comparing the images in Fig. 3 with data in Fig. 2, the molten pool images are also seen to be more sensitive to variations in laser power than to scan velocity. Using constant scan velocity in processing, the geometric shape of the molten pool changes prominently with variation in laser power. When laser power is decreased, the size of the pool shrinks, and the angle at the front end is smaller. In contrast, changing the scan velocity while keeping the laser power constant will cause only a small difference in the pool image. Thus, for surface modification with variable absorbed laser power and scan velocity, images of the pool do not reflect the molten depth very well. However, for constant scan velocity processing (which is the common method in surface modification), such images can provide sufficient feedback of the molten depth for closed-loop control. The key features of the geometric shape of the molten pool for on-line estimation will be analysed and discussed further in the

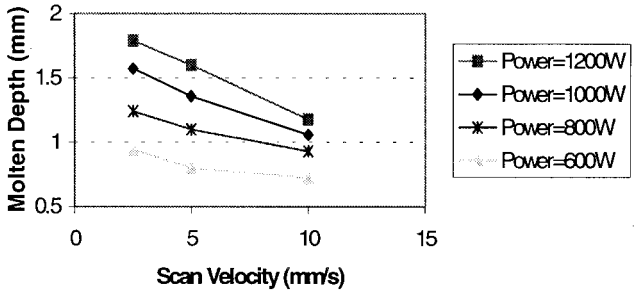

(a) Depth of the modified surface vs. scan velocity for different laser output power.

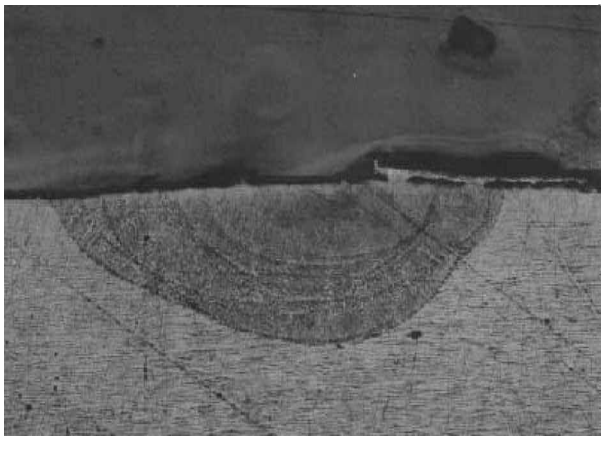

(b) Structure of modified surface.

Fig. 2 Laser surface modification results by constant processing parameters

fourth section. In the following study, it is assumed that constant scan velocity will be utilized during laser processing. In order to obtain molten depth feedback from the molten pool geometric information, a real-time algorithm of image processing will be the next challenge.

3 REAL-TIME ALGORITHM FOR IMAGE PROCESSING

Real-time image processing uses edge detection to simplify the analysis of the image by preserving useful structural information about object boundary. There are several research results on edge detectors (four well-known types are the Canny, Nalwa–Binford, Sarkar–Bowyer and Sobel detectors [**8**]). Owing to the excellent performance of the Canny edge detector (high signal–noise ratio, good edge localization and elimination of multiple response) and the features of the image obtained, the Canny edge detector for step edges is used with modification to serve as the front-end edge detector. Other methods have been tested but cannot provide satisfactory results, so they are not utilized in this study.

In order to decrease the noise effects, Gaussian smoothing is applied to the image first described as

$$I_s = G * I$$

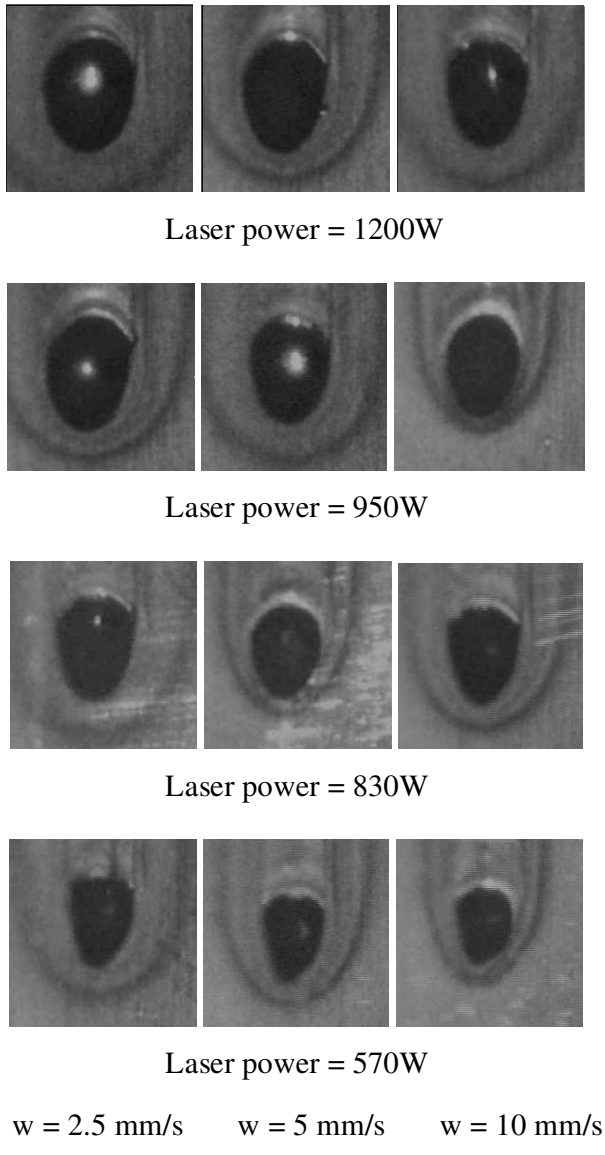

Fig. 3 Images of the molten pool under different laser powers and scan velocities

where G is a two-dimensional Gaussian filter, I represents the image array, and $*$ denotes convolution:

$$G = \exp\left(-\frac{i^2 + j^2}{2\sigma^2}\right)$$

According to Canny [**9**], the first derivative of the Gaussian operator is an efficient approximation of the optimized operator for a step edge with a 20 per cent performance decrease. Thus, the following operation is applied to the result of image smoothing:

$$I_r = G_n * I_s$$

where

$$G_n = \frac{\partial G}{\partial n} = n \cdot \nabla G$$

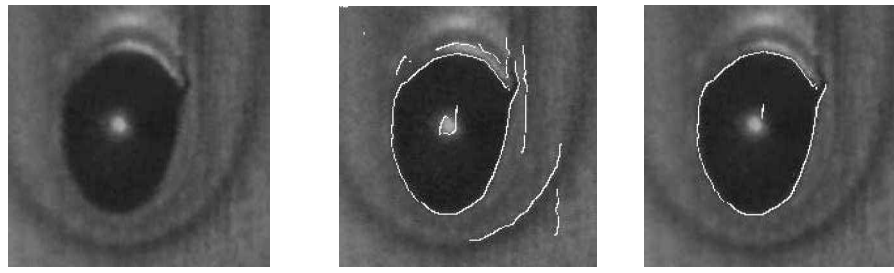

(a) (b) (c)

Fig. 4 Processing result of the edge detector: (a) original molten pool image; (b) middle-stage image processing result; (c) final image processing result

Here, $\boldsymbol{n}$ should be the normal to the direction of an edge to be detected and can be estimated from the smoothed gradient direction

$$\mathrm{n} = \frac{\nabla(G * I)}{|\nabla(G * I)|}$$

An edge candidate, I_e, is a local maximum of I_r. A function, F, of non-maximum suppression is built to substitute for calculating the second derivation Gaussian operator:

$$I_e = F(I_r)$$

Two edge magnitude thresholds, T_{e1} and T_{e2} ($T_{e1} > T_{e2}$), are selected with hysteresis [**9**] to classify I_e and to form the edge set E. The processing result is shown in Fig. 4b.

In order to eliminate the edges caused by the heat affected zone, two grey level thresholds, T_{g1} and T_{g2} ($T_{g1} < T_{g2}$), also with hysteresis, are used, combined with edge magnitude thresholds, based on the original image histogram analysis. The process is defined as follows:

If $I_e(i,j) > T_{e1}$ and $I(i,j) < T_{g1}$, $(i,j) \in E$,
break = FALSE, $i \pm \Delta$, $j \pm \Delta$; Δ is a small increase
If $I_e(i,j) < T_{e2}$ or $I(i,j) > T_{g2}$, $(i,j) \notin E$,
break = TRUE
If $T_{e1} > I_e(i,j) > T_{e2}$ and $T_{g2} > I(i,j) > T_{g1}$ and
break = FALSE, $(i,j) \in E$, otherwise break = TRUE

Figure 4c shows that the extra edges are greatly reduced. The edge set E is the data source of on-line estimation of surface modification depth. The algorithm will take 60 ms to complete the processing for one frame image, which is fast enough for real-time process control.

4 ANALYTICAL MODELS OF LASER SURFACE MODIFICATION

The purpose of on-line estimation is to supply a real-time feedback of the depth of the modified surface from information of the molten pool image, and to direct the controller by giving the relationship between molten depth and controlled processing parameters. Owing to the complicated mechanism of the transient heat process of surface modification and welding, neural networks are usually applied to model the process. Because the key features that are used to train the neural network are critical to the future performance of the model, analytical models are analysed first to find the key features to train the neural network. Also, the approximate effects of controlled processing parameters can be obtained by analysis of the analytical models to direct the controller.

As the laser interacts on the metal surface in a very thin film layer [**10**], laser surface modification can be simplified and modelled as a moving point heat resource on a semi-infinite metal plate without considering the size of the laser spot. The model is described as [**11**]

$$T(x,y,z,t) = \int_0^t \frac{Q\,\mathrm{d}\tau}{[4\pi a(t-\tau)]^{3/2}\rho c_p} \times \exp\left[-\frac{x - w(t-\tau)^2 + y^2 + z^2}{4a(t-\tau)}\right]$$

The temperature field reaches a steady state for $t \to \infty$. In this case the lower limit of the integral equation above leads to the simple expression

$$T(x,y,z) = \frac{Q}{4\pi k r}\exp\left[-\frac{w(r-x)}{2a}\right]$$

In the model above, y and z are symmetric, which means that the width of the molten pool is double the depth of the modified surface. The size of the molten pool in the x direction, which is the same as the direction of movement of the heat source, is affected by the scan velocity. In the following, the correlation between molten depth (also bead width) and laser surface modification processing parameters (laser power absorbed and scan velocity) are explored to show the trend of influence.

Introduce the dimensionless quantities:

$$\Theta = \frac{4\pi k a T}{wQ}, \qquad \xi = \frac{wx}{a}, \qquad \eta = \frac{wy}{a}, \qquad \zeta = \frac{wz}{a}$$

$$\gamma^2 = \eta^2 + \zeta^2$$

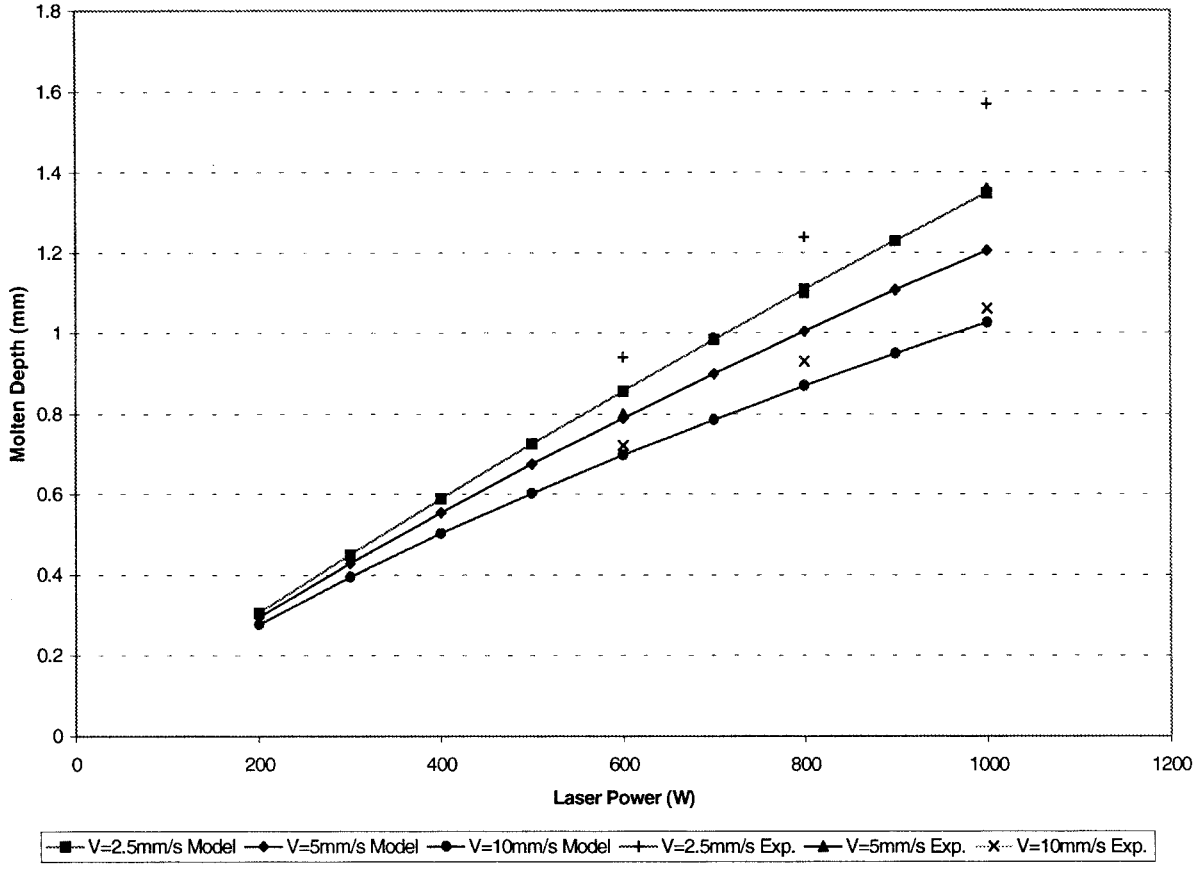

Fig. 5 Relation of laser power and molten depth of moving point heat source model. Properties of steel at 400 °C: $\rho = 7730\,\mathrm{kg/m^3}$, $k = 45\,\mathrm{W/m\,K}$, $c = 600\,\mathrm{J/kg\,K}$, $a = 9.6 \times 10^{-6}\,\mathrm{m^2/s}$, $T_{\mathrm{melting}} = 1470\,^\circ\mathrm{C}$, absorption rate $\varepsilon = 0.65$

and write the solution as [**12**]

$$\theta(\xi, \eta, \zeta) = \frac{\exp\{-0.5[(\xi^2 + \gamma^2)^{1/2} - \xi]\}}{(\xi^2 + \gamma^2)^{1/2}} \tag{1}$$

To calculate bead width, the temperature field on the surface of the block (ξ–η plane) is described by equation (1) with $\gamma = \eta$. The isotherm can be derived from equation (1) by subscribing

$$(\xi^2 + \eta^2)^{1/2} = \mu \tag{2}$$

Then equation (1) can be written as

$$\xi = \mu + 2\ln(\mu\Theta)$$

For the maximum and minimum value of η to obtain the molten depth and bead width,

$$\frac{\partial \eta}{\partial \xi} = \frac{\partial(\mu^2 - \xi^2)^{1/2}}{\partial \xi} = 0$$

$$\frac{\partial \mu}{\partial \xi} = \frac{\xi}{\mu}$$

$$\xi = \frac{\mu^2}{2 + \mu} \tag{3}$$

$$\mu\Theta = \exp\left(\frac{-\mu}{2 + \mu}\right) \tag{4}$$

The molten depth or bead half-width can then be calculated by solving equations (4), (3) and (2).

Figure 5 shows the data of the model for variable laser power and scan velocity compared with experimental data. From the curves it can be concluded that molten depth and bead width are roughly linear to the laser power absorbed. This result is the same as Romer's conclusion [**7**], and can also be observed approximately from the transient experimental data in Figs 6 and 9. The scan velocity has a relatively small influence on molten depth and bead width compared with the laser power, which can also be verified by Fig. 2 from preliminary experiments.

The conclusions from the moving point heat source model can be utilized to build a control model because it provides the trends of variation in molten depth with laser power, but it is not accurate enough for on-line molten depth estimation. Experiment results clearly show that bead width is larger than molten depth. The main reasons for such a difference are the defocusing of the laser beam in the laser surface modification process and the TEM mode of the laser beam. Therefore,

the moving point heat source cannot model the laser beam accurately. The more realistic analytical model is the Gaussian distribution model described as follows [13, 14]:

$$T(x,y,z,t) = \int_0^t \frac{Q(t-\tau)^{1/2}}{\pi\rho c(4\pi a)^{1/2}[2a(t-\tau)+\sigma^2]} \times \exp\left[-\frac{(x-w\tau)^2+y^2}{4a(t-\tau)+2\sigma^2} - \frac{z^2}{4a(t-\tau)}\right] \mathrm{d}\tau$$

where σ has dimensions of length and can be considered as the radius of the defocused laser spot. In this model, y and z are no longer symmetric owing to the size of the laser spot. This model can only be solved numerically. It is quite difficult to find analytically the maximal geometrical value of the molten pool in the y and z directions (molten width and depth). A large number of calculations need to be carried out in order to obtain the boundary of the molten pool to define the relationship between the width of the molten pool and molten depth. Thus, a large amount of calculation results needs to be stored in a table. Searching such a table, which is time consuming, is not feasible for on-line estimation and control.

From both the moving point heat source model and Gaussian distribution model it can be concluded that bead width is a sufficient key feature for the neural network model to predict molten depth. In the Gaussian model, during the transient heat transfer process, because of the laser beam diameter, the energy distribution in the laser beam, and a thin laser–metal interactive layer, the molten pool width can reach a steady state faster than the molten depth. Therefore, the neural network must utilize a time series of molten pool widths as an input vector, considering the transient heat process. The diameter of the defocused laser beam should be kept

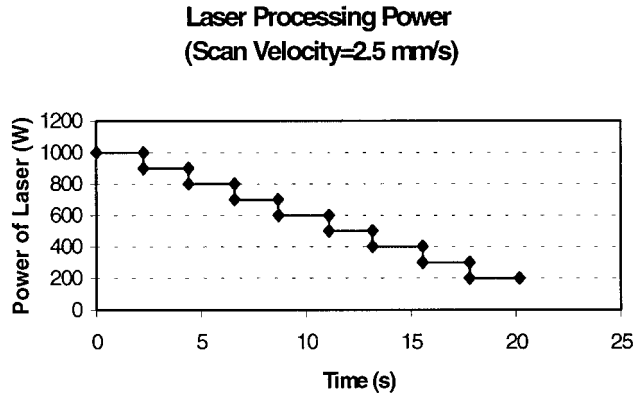

(a) Laser power curve (Step mode).

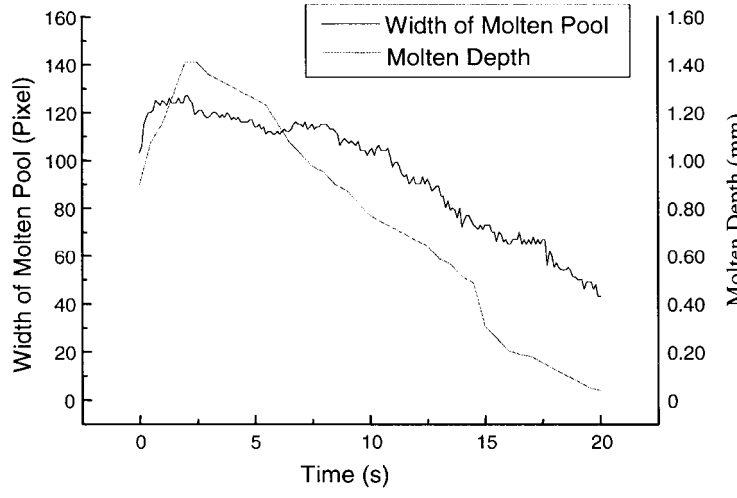

(b) Curves of molten pool width and molten depth.

Fig. 6 Experiment for neural network training

constant, which means the distance between the laser head and the workpiece is a constant.

5 NEURAL NETWORK MODEL FOR ON-LINE ESTIMATION OF MOLTEN POOL

Owing to the performance and limitation of the analytical models mentioned above, a neural network model is introduced for on-line estimation of molten depth. The measured width of the molten pool and molten depth as prototype variables are shown in Fig. 6. The laser is controlled in step mode to simulate the fluctuation of laser power absorbed. The widths and depths of the molten pool are measured by off-line computer vision. The bead is cut along its centreline in order to measure the molten depth. Micrographs (×5) of the samples are scanned into a computer with a 100 d.p.i. (dots per inch) resolution so that 500 measurements can be taken per inch for each sample. The molten widths and depths are outlined and measured using image processing software.

A multilayer perceptron (MLP) neural network can provide a good approximation to arbitrate function. A two-layer MLP neural network is selected to build the model shown in Fig. 7. A log-sigmoid function is applied as the transfer function in both layers. The input vector is a time series of molten pool widths. The output of the neural network is molten depth.

The molten pool width can reach a steady state faster than the molten depth because of the laser beam diameter, the energy distribution in the laser beam and a thin laser–metal interactive layer. For on-line estimation

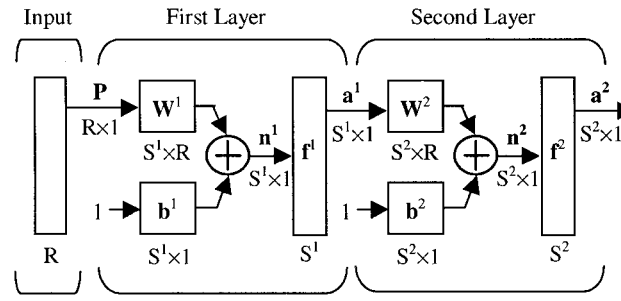

$$a^2=f^2(W^2f^1(W^1P+b^1)+b^2)$$

R=40, S^1=15, S^2=1, f = log-sigmoid (n).

Fig. 7 Multilayer neural network structure

of the molten depth from the width of the molten pools, considering the transient influences, a time series of molten pool widths is used as the input vector of the training prototypes. Assume that the molten depth will be N seconds later than the width of the molten pool in achieving a steady state. The control computer will take $\Delta t = 100$ ms to complete one time feedback control including image grabbing, image processing, geometric parameter extraction, on-line estimation and control signal calculation. Therefore, for the target output (molten depth d) of the neural network at time t, the input vector will be

$$\boldsymbol{P} = [p[\tau-(R-1)\Delta t], p[\tau-(R-2)\Delta t], \ldots, p[\tau]]^{\mathrm{T}}$$

where $p[t]$ is the width of the molten pool at time t, and $R = N \times 10$ to satisfy the assumptions above. In order

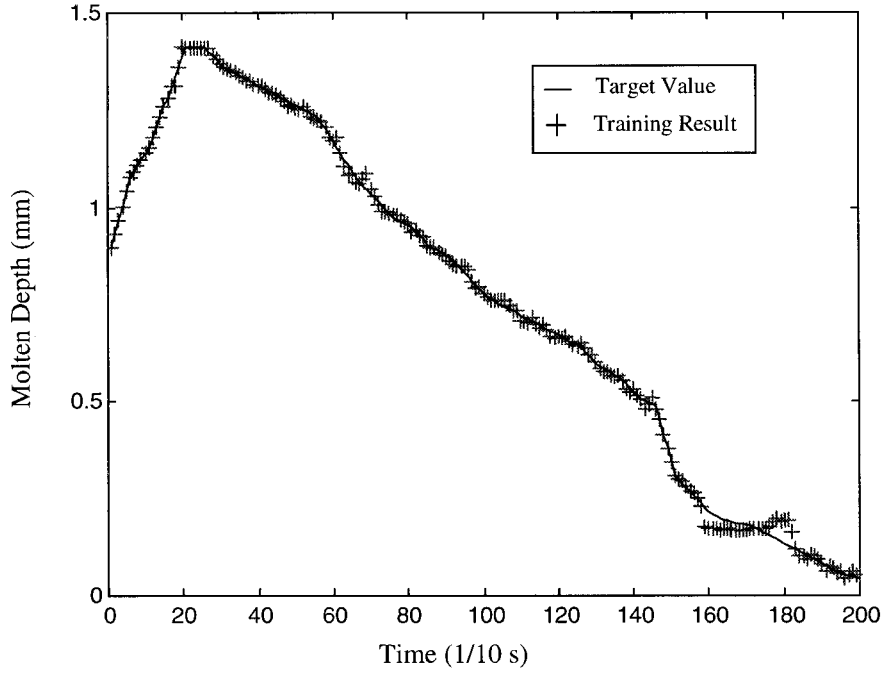

Fig. 8 Comparison of the molten depth target value and training result

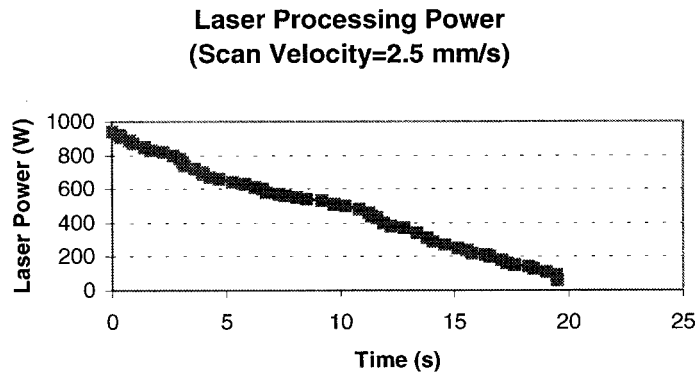

(a) Laser power curve (Linear mode).

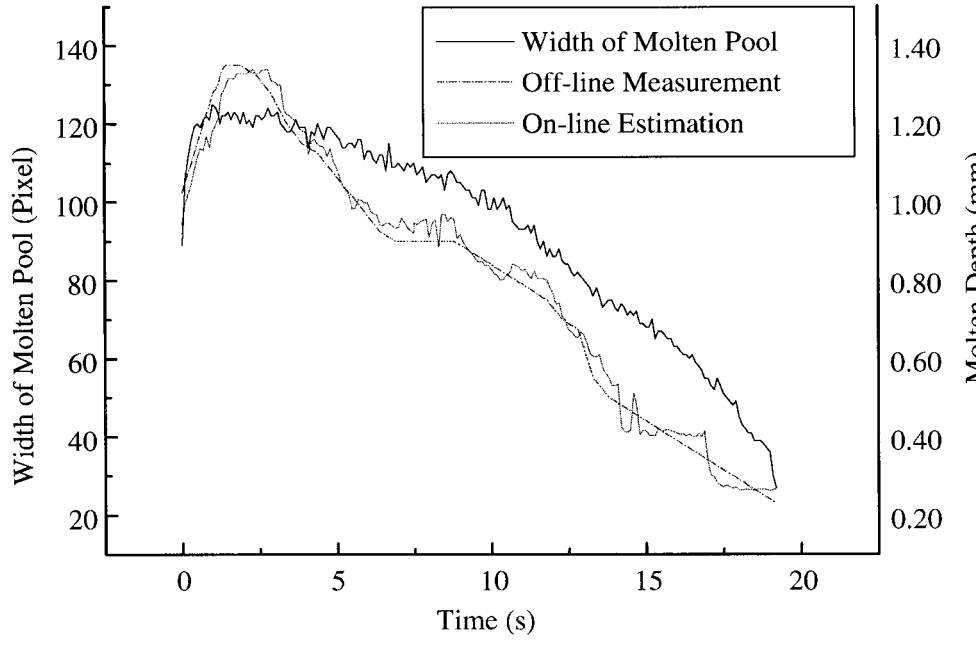

(b) Comparison of on-line estimation and off-line measuring results.

Fig. 9 Verification of the neural network on-line estimation model

to eliminate the noise produced by fluctuation of the molten pool, a larger R than $N \times 10$ is selected as the dimension of the input vector. Here, after training and comparing, $R = 40$ is used in the neural network model.

Back propagation is a well-established method to train an MLP neural network [**15**]. A MATLAB program is developed to follow the back propagation method to train the neural network and optimize the neuron number in the hidden layer according to the convergence speed and error. In order to accelerate the convergence, a variable learning rate and momentum method are applied in the learning algorithm [**15**]. The training prototypes and results are shown in Fig. 8. Comparing the convergence speed and sum-squared error, and in order to reduce the redundant space in the model, $S^1 = 15$ is chosen as the number of neurons in the hidden layer. The sum-squared error of the training is less than 0.01.

The trained neutral network is tested by another experiment result, with linearly changed laser power and the same scan velocity (2.5 mm/s). Figure 9 provides a comparison of experiment and estimation results. The test result shows that, for the same scan velocity, the neural network on-line estimation model can predict modified surface depth quite well.

6 CONCLUSION

Computer imaging is an efficient sensing method for laser surface modification with alloying or remelting. By a

high-speed shutter camera with laser strobe lighting, well-contrasted molten pool images can be acquired, the quality of which is sufficient for sensing. An algorithm for real-time image processing is developed using a modified Canny detector. The algorithm proves to be very robust and high speed. The simplified analytical model of laser surface modification performs an approximate linear relationship between the laser power absorbed and the depth of modified surface. This relationship can be applied in the control model to direct the behaviour of the controller. The width of the molten pools is the key feature for molten depth estimation. A neural network on-line estimation model for molten depth is built considering the transient process of laser processing. Based on an analysis of an analytical model and designed transient process experiments, the model is trained by the back propagation training method, using a time series of molten widths as the input vector. The verification results show that the neural network on-line estimation model can predict the depth of a modified surface very well for the experimental material (AISI 304). Closed-loop control of laser surface modification will be studied on the basis of such sensing and on-line estimation. The sensing, on-line estimation and control method established for stainless steel will be extended to titanium surface modification in future work.

ACKNOWLEDGEMENT

This work was financially supported by the US Department of Education, Grant P200A80806-98.

REFERENCE

1 **Heuvelman, C. J., Konig, W.,** *et al.* Surface treatment techniques by laser beam machining. *Ann. CIRP*, 1992, **41**(2), 657–666.

2 **Romer, G. R. B. E., Hoeksman, M.** and **Meijer, J.** Industrial imaging controls laser surface treatment. *Photonics Spectra*, 1997, **31**(11) 104–109.

3 **Tu, J. F., Lankalapalli, K. N., Gartner, M.** and **Leong, K. H.** On-line estimation of laser weld penetration. *Trans. ASME, J. Dynamic Syst., Measmt Control*, 1997, **119**, 791–801.

4 **Li, L., Qi, N., Brookfield, D. J.** and **Steen, W. M.** On-line laser weld sensing for quality control. *SPIE*, 1990, **1609**, 411–421.

5 **Derouet, H., Coste, F., Sabatier, L.** and **Fabbro, R.** Real time control of surface treatments with liquid phase (molten depth on-line estimation). *SPIE*, 1996, **2789**, 264–272.

6 **Lankalapalli, K. N., Tu, J. F., Leong, K. H.** and **Gartner, M.** Laser weld penetration estimation using temperature measurements. *Trans. ASME, J. Mfg Sci. Engng*, 1999, **121**(2), 179–188.

7 **Romer, G. R. B. E.** and **Meijer, J.** Analytical model describing the relationship between laser power, beam velocity and melt pool depth in the case of laser (re)melting, -alloying and -dispersing. *SPIE*, 1997, **3097**, 507–516.

8 **Heath, M., Sarkar, S., Sanocki, T.** and **Bowyer, K.** Comparison of edge detectors—a methodology and initial study. *Computer Vision and Image Understanding*, 1998, **69**(1), 38–54.

9 **Canny, J.** A computational approach to edge detector. *IEEE Trans. Pattern Analysis Mach. Intell.*, 1986, **PAMI-8**(6), 679–698.

10 **Prokhorov, A. M.** and **Konov, V. I.** *Laser Heating of Metals*, 1990 (Adam Hilger, New York).

11 **Carslaw, H. S.** and **Jaeger, J. C.** *Conduction of Heat in Solids*, 1959 (Oxford Press).

12 **Grigull, U.** and **Sandner, H.** *Heat Conduction*, 1984 (Hemisphere, Washington).

13 **Eagar, T. W.** and **Tsai, N.-S.** Temperature fields produced by traveling distributed heat source. *Weld. J.*, 1983, **62**(12), 346-s–355-s.

14 **Nguyen, N. Y., Uhta, A., Matsuoka, K., Suzuki, N.** and **Maeda, Y.** Analytical solution for transient temperature of semi-infinite body subjected to 3-D moving heat source. *Weld. J.*, 1978, **78**(8), 265-s–274-s.

15 **Hagan, M. T., Demuth, H. B.** and **Beale M.** *Neural Network Design*, 1995 (PWS, Boston, Massachusetts).